Time domain Doppler estimators of the amplitude of vibrating targets

Sung-Rung Huang
Department of Electrical Engineering, University of Rochester, Rochester, New York 14627

Robert M. Lerner
Department of Radiology, University of Rochester, Rochester, New York 14642

Kevin J. Parker
Rochester Center for Biomedical Ultrasound, University of Rochester, Rochester, New York 14627

(Received 9 November 1990; accepted for publication 30 September 1991)

Five basic algorithms using time domain techniques are described in this paper to estimate the amplitude and frequency of relatively low-frequency vibration of a target that is interrogated with a relatively high-frequency wave. The estimations are based on the Doppler shift generated by the vibrating target, which produces a frequency modulated echo. All algorithms presented here use only a small fraction of the low-frequency vibration cycle to obtain the estimated parameters; therefore, real-time imaging of vibration can be made in many applications. The described algorithms complement each other to cover a wide range of the estimated parameters and different sampling, scanning, and imaging criteria. Simulations show that these time domain algorithms have good noise performance and low sensitivity to nonlinearities of the vibration that may be present in nonideal conditions.

PACS numbers: 43.60.Gk, 43.80.Vj

INTRODUCTION

The pulsed Doppler ultrasound technique has been successfully applied for blood flow detection since the 1970s.[1–4] Since then, Doppler spectral parameter estimations using time and frequency domain processing have been extensively studied.[5–13] These methods are oriented toward steady and slowly varying (pulsatile) blood flow, and are not well suited for vibration amplitude detection using Doppler ultrasound. Vibration images are produced in sonoelasticity imaging which was recently developed[14–17] to detect hard tumors surrounded by relatively soft tissues. The principle of sonoelasticity imaging is briefly described as follows: The tissue is vibrated by a low-frequency (compared to the investigating wave) external source; and regions of abnormal elasticity are expected to produce abnormal vibration amplitudes. However, the Doppler spectrum from a vibrating target is symmetric about the center frequency; thus the mean frequency is zero. Therefore, the conventional Doppler velocity estimators are not appropriate for detecting vibration and new approaches are required. Estimators based on time domain processing are proposed in this paper for sonoelasticity imaging and other applications where various kinds of propagating waves, e.g., ultrasound, laser, and microwave, are utilized to detect oscillating structures. Since our estimators need only very few samples of the Doppler signal, asynchronous real-time two-dimensional sonoelasticity imaging or vibration imaging systems can be built with proper design of scanning and gating.

The problem of estimating the vibrational parameters underlies many applications aside from sonoelasticity imaging, e.g., remote sensing, radar, sonar, acoustics, and laser calibration of sound fields. Various estimation methods have been proposed. Since the time domain waveform is complicated, frequency domain techniques have been the primary object of past studies.[16,18–24] Since all the techniques referenced above require the use of long sequences of Doppler signals to avoid frequency aliasing and to achieve noise reduction, they are not as well suited to real-time imaging. Time domain processing which makes use of *a priori* information regarding the nature of the Doppler shifts from vibrating targets requires less data than frequency domain approaches to achieve the same estimation, and, therefore, is more suitable for real-time and/or imaging applications.

Five time domain algorithms are proposed in this paper and the estimated parameters are vibration amplitude and frequency. Four among the five are devoted to estimating vibration amplitude; the other one is a vibration frequency estimator. The theoretical derivations and performances of each estimator will be presented in the following sections. Variations and advantages of the algorithms will also be addressed. The equivalence of baseband and rf domain processing will also be discussed.

I. THEORY

A. Derivation of the Doppler signal for vibrating target

When an incident laser, radio, or acoustic wave is applied to a moving target, the frequency of the detected backscattered signals from that moving target will be Doppler shifted. If the illuminated target is vibrating, the returned signal is more complicated. In this case, the validity and the mathematical formulation of the Doppler shift are still subjects of controversy involving some linear and nonlinear derivations.[25,26] But for the simplified case of a sinusoidally

 0001-4966/92/020965-10$00.80

vibrating target, the returned signal can be represented by a pure-tone frequency modulation (FM) process.

Assume that the scatterers are vibrating with the form

$$\xi(t) = \xi_m \sin(\omega_L t + \varphi_L), \tag{1}$$

$$v(t) = \dot{\xi}(t) = v_m \cos(\omega_L t + \varphi_L), \tag{2}$$

where $\xi(t)$ is the displacement of the vibration, $v(t)$ is the velocity of the vibration, ξ_m is the vibration amplitude of the displacement field, $v_m = \omega_L \xi_m$ is the vibration amplitude of the velocity field, $f_L = \omega_L/2\pi = 1/T_L$ is the vibration frequency, and φ_L is the vibration phase.

Then, the received signal can be written as[18,19]

$$s_r(t) = A \cos\left(\int_{-\infty}^{t} \omega_i(t)dt\right), \tag{3}$$

where $\omega_i(t) = \omega_0 + \omega_d(t)$ is the instantaneous frequency and $\omega_d(t)$ is the Doppler shift of frequency due to the motion of the target. The Doppler shift frequency can be expressed as

$$\omega_d(t) = [2v(t)/c_0]\omega_0 \cos\theta, \tag{4}$$

where c_0 is the propagating speed and θ is the angle between the direction of wave propagation and the direction of vibration. Substituting Eqs. (1) and (2) into Eq. (3), the received signal can be rewritten as a pure-tone FM equation

$$s_r(t) = A \cos[\omega_0 t + \varphi_0 + \beta \sin(\omega_L t + \varphi_L)], \tag{5}$$

where φ_0 is an arbitrary constant phase term. The modulation index of the FM process β is directly related to the vibration amplitude of the velocity or displacement field as follows:

$$\beta = \frac{2v_m\omega_0 \cos\theta}{\omega_L c_0} = \frac{2\xi_m\omega_0 \cos\theta}{c_0} = 4\pi\frac{\xi_m}{\lambda_0}\cos\theta, \tag{6}$$

where λ_0 is the wavelength of the interrogating wave. Thus estimating the modulation index β is equivalent to estimating the vibration amplitude of the displacement and/or velocity fields. The amplitude constant A is assumed to be unity to simplify the analysis for the rest of this paper.

B. Estimation by operations on phases

If synchronous detection is used to detect the Doppler signal, the resulting two discrete quadrature signals can be represented as

$$I_k = \cos[\beta \sin(k\omega_L T_s + \varphi_L) + \varphi_0] \tag{7}$$

and

$$Q_k = \sin[\beta \sin(k\omega_L T_s + \varphi_L) + \varphi_0], \tag{8}$$

where T_s is the sampling period and k is the sample number: 1,2,3... . In practice, if pulse Doppler ultrasound is used, the sampling period T_s is determined by the pulse repetition rate f_r.

Noting that the cross products of two quadrature sinusoidal signals can be simplified using trigonometric identities, two useful signals are defined as follows:

$$\begin{aligned}\phi_k &\equiv \tan^{-1}(I_k Q_{k-1} - I_{k-1}Q_k)/(I_k I_{k-1} + Q_k Q_{k-1}) \\ &= -([\beta \sin(k\omega_L T_s + \varphi_L) + \varphi_0] \\ &\quad - \{\beta \sin[(k-1)\omega_L T_s + \varphi_L] + \varphi_0\}) \\ &= -2\beta \cos(k\omega_L T_s - \omega_L T_s/2 + \varphi_L) \sin(\omega_L T_s/2)\end{aligned} \tag{9}$$

and

$$\begin{aligned}\phi'_k &\equiv \tan^{-1}(I_k Q_{k-1} + I_{k-1}Q_k)/(I_k I_{k-1} - Q_k Q_{k-1}) \\ &= [\beta \sin(k\omega_L T_s + \varphi_L) + \varphi_0] \\ &\quad + \{\beta \sin[(k-1)\omega_L T_s + \varphi_L] + \varphi_0\} \\ &= 2\beta \sin(k\omega_L T_s - \omega_L T_s/2 + \varphi_L) \cos(\omega_L T_s/2) + 2\varphi_0.\end{aligned} \tag{10}$$

These two signals are called phase and co-phase signals, respectively, in this paper. They are both related to the phase of the received signal and form the basis for the following estimations. Derivations of these two signals involve the complex multiplications of two successive complex quadrature signals. Examining these two signals closely, they are 90 deg out-of-phase with different amplitude multipliers. In other words, they are the phase shifted and amplified version of the vibration signals. Figure 1(a) shows the simulated waveform of the two quadrature signals with 30-dB signal-to-noise ratio and small modulation index $\beta = 0.5$. The corresponding estimations of the phase and co-phase signals are shown in Fig. 1(b).

To estimate the vibration amplitude, note that the sum and the difference of successive samples of the phase signal can be written in the forms

$$\begin{aligned}\phi_k^- &\equiv \phi_k - \phi_{k-1} \\ &= 4\beta \sin[(k-1)\omega_L T_s + \varphi_L] \\ &\quad \times \sin(\omega_L T_s/2)\sin(\omega_L T_s/2),\end{aligned} \tag{11}$$

$$\begin{aligned}\phi_k^+ &\equiv \phi_k + \phi_{k-1} \\ &= -4\beta \cos[(k-1)\omega_L T_s + \varphi_L] \\ &\quad \times \cos(\omega_L T_s/2)\sin(\omega_L T_s/2).\end{aligned} \tag{12}$$

Similarly, the sum and difference of successive co-phase samples give

$$\begin{aligned}\phi'^{-}_k &\equiv \phi'_k - \phi'_{k-1} \\ &= 4\beta \cos[(k-1)\omega_L T_s + \varphi_L] \sin(\omega_L T_s/2) \\ &\quad \times \cos(\omega_L T_s/2),\end{aligned} \tag{13}$$

$$\begin{aligned}\phi'^{+}_k &\equiv \phi'_k + \phi'_{k-1} \\ &= 4\beta \sin[(k-1)\omega_L T_s + \varphi_L] \\ &\quad \times \cos\left(\frac{\omega_L T_s}{2}\right)\cos\left(\frac{\omega_L T_s}{2}\right) + 4\varphi_0.\end{aligned} \tag{14}$$

If the vibration frequency is known, the vibration amplitude can be estimated directly from the above equations:

$$\hat{\beta}_1 \equiv \sqrt{\frac{[\phi_k^- \cos(\omega_L T_s/2)]^2 + [\phi_k^+ \sin(\omega_L T_s/2)]^2}{4\sin^2(\omega_L T_s)\sin^2(\omega_L T_s/2)}}. \tag{15}$$

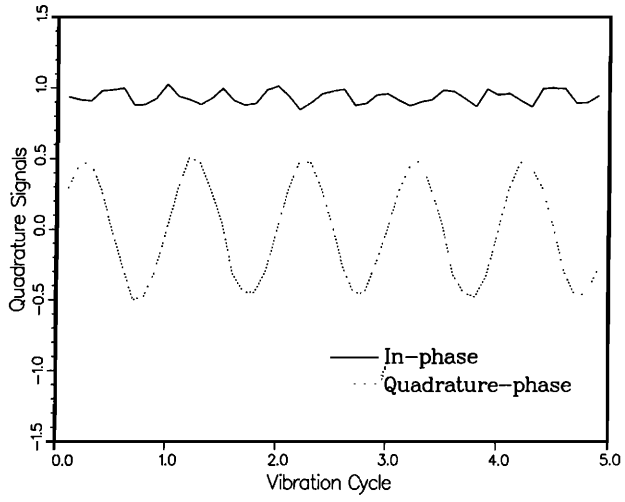

(a)

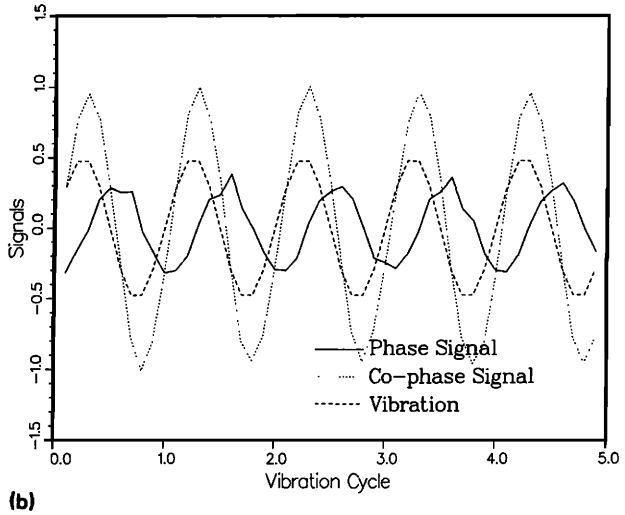

(b)

FIG. 1. (a) Time domain waveforms of two quadrature signals I_k and Q_k; (b) the phase signal ϕ_k, co-phase signal ϕ'_k, and vibration $v_k \equiv \beta \sin(k\omega_L T_s + \varphi_L)$. Signal-to-noise ratio is 30 dB, the modulation index is $\beta = 0.5$, and the sampling frequency is $f_s = 10 f_L$.

This estimator will be referred as successive-phase estimator. Notice that the carrier phase φ_0 does not appear throughout the derivation as only phase samples are used, and, therefore, this estimation is independent of the unknown carrier phase.

Since the sum and difference of successive phase and co-phase signals are essentially similar, one can obtain the same estimation using the sum and difference of the two successive samples of the co-phase signal as shown below

$$\hat{\beta}'_1 \equiv \sqrt{\frac{[\phi'^{-}_k \cos(\omega_L T_s/2)]^2 + [\phi'^{+}_k \sin(\omega_L T_s/2)]^2}{4 \sin^2(\omega_L T_s) \cos^2(\omega_L T_s/2)}}. \tag{16}$$

The unknown carrier phase φ_0 in ϕ'^{+}_k [(Eq. (14)] produces a bias in the estimate of β using Eq. (16). The constant phase term can be removed by first filtering ϕ'_k or ϕ'^{+}_k before making further calculations. But in general, this estimation [(Eq. (16)] is inferior to the previous one [(Eq. (15)].

If both phase and co-phase signals are available, the estimation can be achieved by combining these two signals in the following way

$$\hat{\beta}_2 \equiv \sqrt{\frac{[\phi_k / \sin(\omega_L T_s/2)]^2 + [\phi'_k / \cos(\omega_L T_s/2)]^2}{4}}. \tag{17}$$

Since both phase and co-phase signals have contributions depending on the sampling rate, this estimator is called bi-phase estimator. It needs one more arctangent operation than the previous one but is less sensitive to the variation of the sampling rate. Notice that the weightings of phase signal ϕ_k and co-phase ϕ'_k depend on the product of sampling period and vibration frequency. Using the example of $f_s = 10$ kHz and $f_L = 200$ Hz, the resulting argument for the sine and cosine functions is $\pi/50$. This means that the contribution of the co-phase signal is only a correction term and much less than that of a phase signal. Looking back at the phase signal in Eq. (9), the squaring operation gives one dc term which is proportional to the square of the desired parameter β and another term oscillating at twice the vibration frequency. The co-phase signal is used to compensate the rapidly oscillating term. This compensation is not necessarily when the sampling frequency is very high as in the case of conventional Doppler estimators. Once again, since the compensating co-phase term contains a dc unknown carrier phase contribution, either low-pass filtering or calibration is needed to reduce the bias.

If white noise is added to the quadrature signals, the autocorrelation and cross correlation of the noise components at one delay will approach zero. This noise reduction is achieved during the above estimation process by the cross multiplications of in-phase and quadrature-phase signals (I_k and Q_k) to derive the phase and co-phase signals if uncorrelated noise terms are inserted into Eqs. (7) and (8) to produce Eqs. (9) and (10). Applying the same noise reduction technique, the cross products of phase and co-phase signals can be used to achieve more noise reduction in the following forms:

$$\hat{\beta}_3 \equiv \sqrt{(\phi_k \phi'_{k-1} - \phi_{k-1} \phi'_k)/2 \sin^2(\omega_L T_s)}, \tag{18}$$

$$\hat{\beta}'_3 \equiv \sqrt{(\phi_k \phi'_{k-n} - \phi_{k-n} \phi'_k)/2 \sin(n\omega_L T_s) \sin(\omega_L T_s)}. \tag{19}$$

They are termed the one-shift cross-phase estimator and n-shift cross-phase estimator, respectively. The performance of the n-shift cross-phase estimator is similar to that of the one-shift cross-phase estimator but it can be used in more flexible sampling conditions and scanning patterns to achieve the real-time imaging requirement.

In all of the above estimations, the vibration frequency must be known before the vibration amplitude is estimated. In some applications, the vibration source is externally applied and the vibration frequency can be tracked accurately and precisely using a frequency meter, e.g., in sonoelasticity imaging and laser calibration and measurement of sound fields. But in some other applications, e.g., the study of heart valve vibration, the frequency of vibration is an unknown and possibly important parameter. Therefore, an estimation of the vibration frequency may be required. However, we

point out that the estimation of one more parameter out of the same set of sample data will generally increase the variance of the results.

Taking the ratio of difference of the phase and the sum of the co-phase signals and assuming $\varphi_0 = 0$, we have

$$\frac{\phi_k - \phi_{k-1}}{\phi'_k + \phi'_{k-1}} = \frac{4\beta \sin[(k-1)\omega_L T_s + \varphi_L] \sin^2(\omega_L T_s/2)}{4\beta \sin[(k-1)\omega_L T_s + \varphi_L] \cos^2(\omega_L T_s/2)} = \tan^{-2}(\omega_L T_s/2). \quad (20)$$

From the above equation, it is not difficult to derive the phase-ratio estimator for vibration frequency:

$$\hat{f}_L = \left[\tan^{-1}\sqrt{(\phi_k - \phi_{k-1})/(\phi'_k + \phi'_{k-1})}\right]/\pi T_s. \quad (21)$$

Since the vibration frequency is a much slower varying quantity, it is not difficult to remove the unknown carrier phase φ_0 by filtering.

C. Estimation by correlations

Since all the previous algorithms use a fixed number of samples to estimate the parameters, noise performance can only be improved by averaging over the estimated parameters. However, the noise may be amplified in the process of taking trigonometric functions; therefore, the performance improvement is limited to some extent. Given a small modulation index β, noise can cause serious problems in the previous estimators. Thus we seek the development of alternative method estimations, which employ averaging over the raw data.

Returning to the pure-tone FM signal, the spectrum of this signal is well known to be a series of Bessel functions.[27] Therefore, if $x(t)$ represents the complex quadrature signal

$$\begin{aligned} x(t) &= \cos[\beta \sin(\omega_L t + \varphi_L) + \varphi_0] \\ &\quad + i \sin[\beta \sin(\omega_L t + \varphi_L) + \varphi_0] \\ &= e^{i\varphi_0} e^{i\beta \sin(\omega_L t + \varphi_L)} \\ &= e^{i\varphi_0} \sum_{n=-\infty}^{\infty} J_n(\beta) e^{in(\omega_L t + \varphi_L)}, \end{aligned} \quad (22)$$

then the Fourier transform of $x(t)$ will be

$$\begin{aligned} X(\omega) &\equiv \mathcal{F}\{x(t)\} \\ &= \int_{-\infty}^{\infty} x(t) e^{-i\omega t}\, dt, \\ &= 2\pi e^{i\varphi_0} \sum_{n=-\infty}^{\infty} J_n(\beta) e^{in\varphi_L} \delta(\omega - n\omega_L), \end{aligned} \quad (23)$$

where $J_n(\beta)$ is the nth order Bessel function of the first kind.

Let $R_{xx}(\tau)$ be the autocorrelation function of $x(t)$,

$$R_{xx}(\tau) \equiv \frac{1}{T} \int_T x(t+\tau) x^*(t)\, dt, \quad (24)$$

then, from the properties of Fourier transformation, we have

$$\begin{aligned} R_{xx}(\tau) &= \mathcal{F}^{-1}\{X(\omega) X^*(\omega)\} \\ &= \frac{1}{2\pi} \int_{-\infty}^{\infty} 2\pi e^{i(\varphi_0 - \varphi_0)} \\ &\quad \times \sum_{n=-\infty}^{\infty} J_n^2(\beta) e^{in(\varphi_L - \varphi_L)} \delta(\omega - n\omega_L) e^{i\omega\tau}\, d\omega \\ &= \sum_{n=-\infty}^{\infty} J_n^2(\beta) e^{in\omega_L \tau}. \end{aligned} \quad (25)$$

Notice that the unknown carrier phase φ_0 and vibration phase φ_L have been canceled and the resulting power spectrum is independent of those phases.

This autocorrelation function is a series of squared Bessel functions weighted by a complex exponential function and can be evaluated with the aid of the generating function of the Bessel function and z-transform theory as follows: If we replace the term $e^{i\omega_L \tau}$ by z^{-1}, the autocorrelation function can be written into a z transform of a discrete sequence of squared Bessel function as

$$R_{xx}(\tau) = \sum_{n=-\infty}^{\infty} z^{-n} J_n^2(\beta) \quad (26)$$

or the product of two identical discrete Bessel sequences. But the z transform of a discrete Bessel sequence is its generating function, i.e.,

$$\mathcal{T}(\beta, z) \equiv \sum_{n=-\infty}^{\infty} z^{-n} J_n(\beta) = e^{-(\beta/2)(z - 1/z)}. \quad (27)$$

This analytic expression of the Bessel generating function can be found in many mathematical handbooks, e.g., see Ref. 28. It is used to relate the z transform of a Bessel sequence instead of solving differential equations in this derivation. Since the multiplication in the index domain for two discrete sequences is equivalent to the complex convolution in the transform (or z) domain, we have

$$R_{xx}(\tau) = \frac{1}{2\pi i} \oint \mathcal{T}(\beta, \nu) \mathcal{T}\left(\beta, \frac{z}{\nu}\right) \nu^{-1}\, d\nu \Big|_{z = e^{-i\omega_L \tau}}. \quad (28)$$

Evaluating the integral on the unit circle by setting $\nu = e^{i\theta}$, we have

$$\begin{aligned} R_{xx}(\tau) &= \frac{1}{2\pi i} \int_{-\pi}^{\pi} \left[\exp\left(-\frac{\beta}{2}(e^{i\theta} - e^{-i\theta})\right)\right] \\ &\quad \times \left[\exp\left(-\frac{\beta}{2}(e^{i(\theta - \omega_L\tau)} - e^{-i(\theta - \omega_L\tau)})\right)\right] \\ &\quad \times (e^{-i\theta})(ie^{i\theta}\, d\theta) \\ &= \frac{1}{2\pi} \int_{-\pi}^{\pi} \exp\{-\beta[\cos\theta \\ &\quad - \cos(\theta - \omega_L \tau)]\}\, d\theta \\ &= \frac{1}{2\pi} \int_{-\pi}^{\pi} \exp\left[2\beta \sin\left(\frac{\omega_L \tau}{2}\right) \sin\left(\theta - \frac{\omega_L \tau}{2}\right)\right] d\theta \\ &= J_0[2\beta \sin(\omega_L \tau/2)]. \end{aligned} \quad (29)$$

Middleton[29] has derived a similar but incorrect expression for pure-tone FM autocorrelation function, where a cosine was used in place of the sine in the argument.

Since the zeroth-order Bessel function $J_0(x)$ has a series expansion of the form

$$J_0(x) = 1 - \frac{x^2}{2^2} + \frac{x^4}{2^2 4^2} - \frac{x^6}{2^2 4^2 6^2} + \cdots, \tag{30}$$

the autocorrelation function can be approximated as

$$R_{xx}(\tau) \approx 1 - 4\beta^2 \sin^2(\omega_L \tau/2)/4, \tag{31}$$

the desired vibration amplitude can be estimated as

$$\hat{\beta}_4 \equiv \sqrt{[1 - |R_{xx}(T_s)|]/\sin^2(\omega_L T_s/2)}, \tag{32}$$

when the estimated parameter β is small. This is called the autocorrelation estimator for the vibration amplitude.

The autocorrelation function, in practice, is approximated by a finite series:

$$R_{xx}(k,T_s) \approx \frac{1}{N} \sum_{n=0}^{N-1} x_{k-n} x_{k-n-1}^*, \tag{33}$$

where x_k is the discrete complex quadrature signal

$$x_k = \cos[\beta \sin(k\omega_L T_s + \varphi)] + i \sin[\beta \sin(k\omega_L T_s + \varphi)]$$
$$= I_k + iQ_k. \tag{34}$$

The time delay variable τ is replaced by two variables: index k and T_s to emphasize the controllability of the two independent parameters N and T_s. The parameter N can be varied according to real conditions, e.g., sampling rate, noise level, and synchronization. The longer the sequence is used to approximate the autocorrelation, the better the estimation is. In practice, five to ten samples can be used to produce good approximation.

The vibration frequency is assumed to be known in the above estimation. If the vibration frequency is unknown, the estimation can proceed with the aid of the quasiautocorrelation function defined as

$$R'_{xx}(\tau) \equiv \frac{1}{T} \int_T x(t+\tau) x(t) dt. \tag{35}$$

Note that $x(t)$ is complex in the above expression. Then, again the Fourier transform properties give

$$R'_{xx}(\tau) = \mathcal{F}^{-1}\{X(\omega)X(-\omega)\}$$
$$= e^{i2\varphi_0} \sum_{n=-\infty}^{\infty} J_n(\beta) J_{-n}(\beta) e^{in\omega_L \tau}. \tag{36}$$

Using similar mathematical techniques as before, the quasiautocorrelation function can be evaluated to be

$$|R'_{xx}(\tau)| = |e^{i2\varphi_0}| J_0[2\beta \cos(\omega_L \tau/2)]$$
$$\approx 1 - 4\beta^2 \cos^2(\omega_L \tau/2)/4. \tag{37}$$

From the above expression, the quasiautocorrelation estimator can be written immediately as

$$\hat{\beta}'_4 \equiv \sqrt{[1 - |R'_{xx}(T_s)|]/\cos^2(\omega_L T_s/2)}. \tag{38}$$

Since this estimator has the same structure as the autocorrelation estimator, their performance and limitations are basically the same. Notice that the quasiautocorrelation for a continuous, random bandpass process is identically zero[30] in the limit, but the signal we are dealing with is discrete, deterministic, and sample limited and therefore the quasiautocorrelation is not equal to zero.

In cases where the vibration frequency is unknown, the dependence on vibration frequency ω_L can be canceled by summing the autocorrelation (31) and quasiautocorrelation functions (37) as follows:

$$\hat{\beta}''_4 = \sqrt{2 - |R_{xx}(T_s)| - |R'_{xx}(T_s)|}. \tag{39}$$

Since both autocorrelation and quasiautocorrelation functions are used in deriving the estimated parameter, it is called the dual-autocorrelation estimator. This estimation is valid only for small vibration amplitude but holds for all vibration frequency and sampling rates. The performance is again dependent on the length of the sequence used in calculating the two correlation functions.

D. Estimation using the rf signal

The signal processing based upon the phase operation can also be implemented in the radio frequency (rf) domain. This follows the observations

$$\phi_{k,\mathrm{rf}} = \tan^{-1}\left(\frac{I_{k,\mathrm{rf}} Q_{k-1,\mathrm{rf}} - I_{k-1,\mathrm{rf}} Q_{k,\mathrm{rf}}}{(I_{k,\mathrm{rf}} I_{k-1,\mathrm{rf}} + Q_{k,\mathrm{rf}} Q_{k-1,\mathrm{rf}})}\right)$$
$$= -([k\omega_0 T_s + \varphi_0 + \beta \sin(k\omega_L T_s + \varphi_L)]$$
$$- \{(k-1)\omega_0 T_s + \varphi_0$$
$$+ \beta \sin[(k-1)\omega_L T_s + \varphi_L]\})$$
$$= \phi_k - \omega_0 T_s \tag{40}$$

and

$$\phi'_{k,\mathrm{rf}} = \tan^{-1}\left(\frac{I_{k,\mathrm{rf}} Q_{k-1,\mathrm{rf}} + I_{k-1,\mathrm{rf}} Q_{k,\mathrm{rf}}}{I_{k,\mathrm{rf}} I_{k-1,\mathrm{rf}} - Q_{k,\mathrm{rf}} Q_{k-1,\mathrm{rf}}}\right)$$
$$= [k\omega_0 T_s + \varphi_0 + \beta \sin(k\omega_L T_s + \varphi_L)]$$
$$+ \{(k-1)\omega_0 T_s + \varphi_0$$
$$+ \beta \sin[(k-1)\omega_L T_s + \varphi_L]\}$$
$$= \phi'_k + 2k\omega_0 T_s - \omega_0 T_s, \tag{41}$$

where $\phi_{k,\mathrm{rf}}$ and $\phi'_{k,\mathrm{rf}}$ are the phase and co-phase signals derived from the rf quadrature signals, i.e.,

$$I_{k,\mathrm{rf}} = \cos[k\omega_0 T_s + \varphi_0 + \beta \sin(k\omega_L T_s + \varphi_L)] \tag{42}$$

and

$$Q_{k,\mathrm{rf}} = \sin[k\omega_0 T_s + \varphi_0 + \beta \sin(k\omega_L T_s + \varphi_L)]. \tag{43}$$

These two rf quadrature signals can be derived from two rf phase shifters with 90-deg phase difference. Another way to obtain the quadrature signals pair from a single component is to take the Hilbert transform. This is in contrast to the usual way of obtaining the baseband quadrature signals by mixing the received rf signals with the rf carrier. Note that an arctangent operation would be used to obtain the phase and co-phase signals from I_{rf} and Q_{rf}; thus the additive term $2k\omega_0 T_s$ in Eq. (41) leads to a rapid oscillation in co-phase and can be eliminated by low-pass filtering. The dc term in both expressions can be removed also. Therefore, all vibration estimators based on the phase operations as described earlier have their own associate rf processing schemes.

The correlation estimator can also be implemented in the rf domain when the baseband quadrature signals are un-

available and only the rf signal is available. Let $z(t) = x(t)e^{i\omega_0 t}$ be the rf signal, where $x(t)$ is the complex signal as defined in Eq. (22); then the Fourier transform of $z(t)$ is simply a shifted version of the Fourier transform of $x(t)$, i.e., $Z(\omega) = X(\omega - \omega_0)$. Therefore, the autocorrelation and quasiautocorrelation functions of $z(t)$ can be expressed as

$$\begin{aligned} R_{zz}(\tau) &= R_{xx}(\tau)e^{-i\omega_0\tau} \\ &= J_0[2\beta \sin(\omega_L\tau/2)]e^{-i\omega_0\tau} \\ &\approx [1-\beta^2 \sin^2(\omega_L\tau/2)]e^{-i\omega_0\tau} \end{aligned} \tag{44}$$

and

$$\begin{aligned} R'_{zz}(\tau) &= R'_{xx}(\tau)e^{i\omega_0\tau} \\ &= J_0[2\beta \cos(\omega_L\tau/2)]e^{i\omega_0\tau} \\ &\approx [1-\beta^2 \cos^2(\omega_L\tau/2)]e^{i\omega_0\tau}, \end{aligned} \tag{45}$$

respectively. Note that $\omega_L T_s \ll \pi$ since high sampling rate is used. In this case, $\cos^2(\omega_L T_s/2) > > > \sin^2(\omega_L T_s/2)$ and, therefore, the quasiautocorrelation approach is less sensitive to noise than the autocorrelation approach.

If the rf sampling rate is sufficiently high, i.e., $\omega_0 T_s \ll \pi$, the vibration estimation can be achieved as described in the previous section. In case the sampling frequency is not sufficiently high or only the real rf signal (either sine or cosine or a phase shifted sine component) is available, the vibration can still be estimated after correction of the $\sin(\omega_0 T_s)$ and/or $\cos(\omega_0 T_s)$ factors. For instance, let $z_1(t) = [z(t) + z^*(t)]/2 = \cos[\omega_0 t + \beta \sin(\omega_L t)]$ be the rf signal; then the autocorrelation of $z_1(t)$ can be expressed as

$$\begin{aligned} &R_{z_1 z_1}(\tau) \\ &= \frac{1}{T}\int_T \left[\left(\frac{z(t+\tau)+z^*(t+\tau)}{2}\right)\left(\frac{z^*(t)+z(t)}{2}\right)\right]dt \\ &= \frac{1}{2}\left[\left(\frac{R_{zz}(\tau)+R^*_{zz}(\tau)}{2}\right)+\left(\frac{R'_{zz}(\tau)+R'^*_{zz}(\tau)}{2}\right)\right] \\ &= \frac{1}{2}\left\{J_0\left[2\beta \sin\left(\frac{\omega_L\tau}{2}\right)\right]\right. \\ &\quad \left. + J_0\left[2\beta \cos\left(\frac{\omega_L\tau}{2}\right)\right]\right\}\cos(\omega_0\tau) \\ &\approx \tfrac{1}{2}(2-\beta^2)\cos(\omega_0\tau) \end{aligned} \tag{46}$$

for $\beta \ll 1$ and $\omega_L\tau \ll \pi$.

This equivalence of signal processing in the baseband and the rf domain gives freedom and high flexibility in design of system architecture, electronic circuitry, and signal processing.

E. Estimation using conventional Doppler estimators

Assuming a target is slowly vibrating with sinusoidal velocity, the output of a short time, mean Doppler frequency estimator is also a sinusoidal function. The frequency of this sinusoid is the vibration frequency and the amplitude is proportional to the modulation index or vibration amplitude. Therefore, one can also upgrade a conventional Doppler estimator with some modifications to estimate the vibration amplitude. But due to the nature of the truncated sinusoid, large bias or variance of the resulting estimates of the sinusoidal amplitude are often encountered. Thus, to reduce the bias and variance, the estimation time can be made longer than that of the estimation techniques proposed in the previous section. It is worthwhile discussing some general approaches to modify a conventional Doppler into vibration Doppler estimates.

The first way to find the amplitude of the sinusoid is to differentiate or to integrate the oscillating estimate. Let the conventional Doppler frequency estimate be $y(t) = \beta \cos(\omega_L t + \varphi_L)$, then $dy(t)/dt = -\omega_L \beta \sin(\omega_L t + \varphi_L)$ and $\int y(t)dt = \beta/\omega_L \sin(\omega_L t + \varphi_L)$. Therefore, the vibration amplitude can be estimated as

$$\beta = \left[y^2(t) + \frac{1}{\omega_L^2}\left(\frac{dy(t)}{dt}\right)^2\right]^{1/2} \tag{47}$$

or

$$\beta = \left[y^2(t) + \omega_L^2\left(\int y(t)dt\right)^2\right]^{1/2}. \tag{48}$$

This method is very general but the performance depends on how well the time derivative or integration can be achieved or be independently estimated. The time derivative and integration terms can be either derived from the conventional Doppler estimate or directly derived from the rf signal. For direct rf estimation, this translates to the use of displacement, velocity, and/or acceleration estimators. For example, since the time shift of the rf correlation peak between successive pulses is proportional to the displacement, and velocity can be derived from the amount of time shift of the rf correlation peak in a few successive pulses,[11] these two signals can be combined to estimate the vibration amplitude.

The other straightforward approach is to use spectral estimation techniques, e.g., see Ref. 31, to estimate the power or amplitude of a truncated sinusoid. Among those spectral estimation techniques, the AR (autoregressive) and ARMA (autoregressive and moving average) models suffer from the stochastic nature of the modeling and, therefore, the resulting estimates are oscillating as a function of truncation length, initial phase of the sampled sinusoid, sampling frequency, etc. Therefore, the sampling must be held at a certain fixed operating point and the vibration frequency can not be changed or swept during the estimation. This will restrict the use of the vibration and the scanning. Some other methods that employ sinusoidal models might perform better. Examples are Pisarenko harmonic decomposition and Prony spectral line estimation.[31] Since the phase of the estimated sinusoid is lost in the Pisarenko method, the signal must be sampled carefully. For all spectral estimation techniques, the major disadvantage is the intensive computation involved in the least-square minimization.

II. RESULTS AND DISCUSSIONS

A. Noise performance of vibration amplitude estimators

Computer simulations suggest that the estimators described above have reasonable noise performance. Figure 2

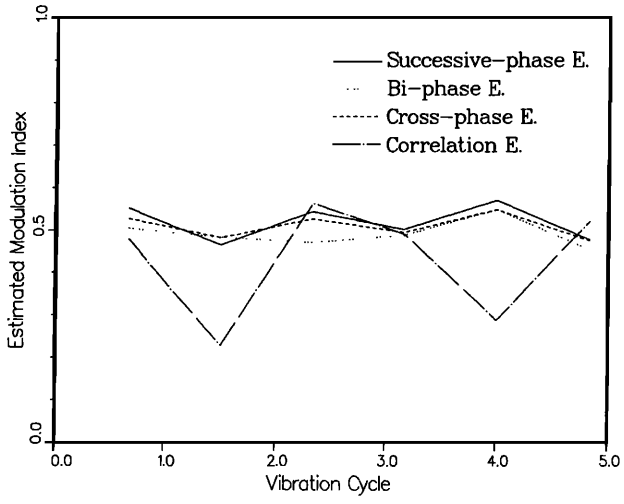

FIG. 2. Typical vibration amplitude for five vibration cycles. Signal-to-noise ratio is 30 dB, the true modulation index is $\beta = 0.5$, and the sampling frequency is $f_s = 6f_L$.

shows the estimated parameters against time. For estimators $\hat{\beta}_1, \hat{\beta}_2, \hat{\beta}_3$, and $\hat{\beta}_4$, sampling rates are fixed at $f_s = 6f_L$ and random noise is added in both quadrature signals to maintain 30 dB signal-to-noise ratio. Other variant estimators ($\hat{\beta}_1', \hat{\beta}_3', \hat{\beta}_4'$, and $\hat{\beta}_4''$) have similar performances to the corresponding estimators and are not shown on the graphs. The true modulation index is $\beta = 0.5$ in this simulation. The results indicate that the estimators are not strongly dependent on the phase of the vibration, and simulations that use nonintegral sampling frequency give similar results. Therefore, synchronized sampling is not necessary. The estimations over signal-to-noise ratio from 10 to 40 dB for three different modulation indices $\beta = 3$, 0.5, and 0.05 are shown in Fig. 3(a). In this case the sampling frequency is again fixed at $f_s = 6f_L$. The results show that cross-phase estimators and correlation estimators ($\hat{\beta}_3$ and $\hat{\beta}_4$) are good for small vibration amplitudes. This is as expected since the small modulation index approximation is involved in the derivations of correlation estimators. But the successive-phase estimator and the biphase estimator ($\hat{\beta}_1$ and $\hat{\beta}_2$) are fairly good over a wide range. Figure 3(b) indicates that the successive-phase estimator can make accurate estimation even when the modulation index is as large as $\beta = 100$ if the sampling rate is maintained within a certain criterion ($f_s = 2.4\beta f_L$ in this simulation), which will be discussed in the next section.

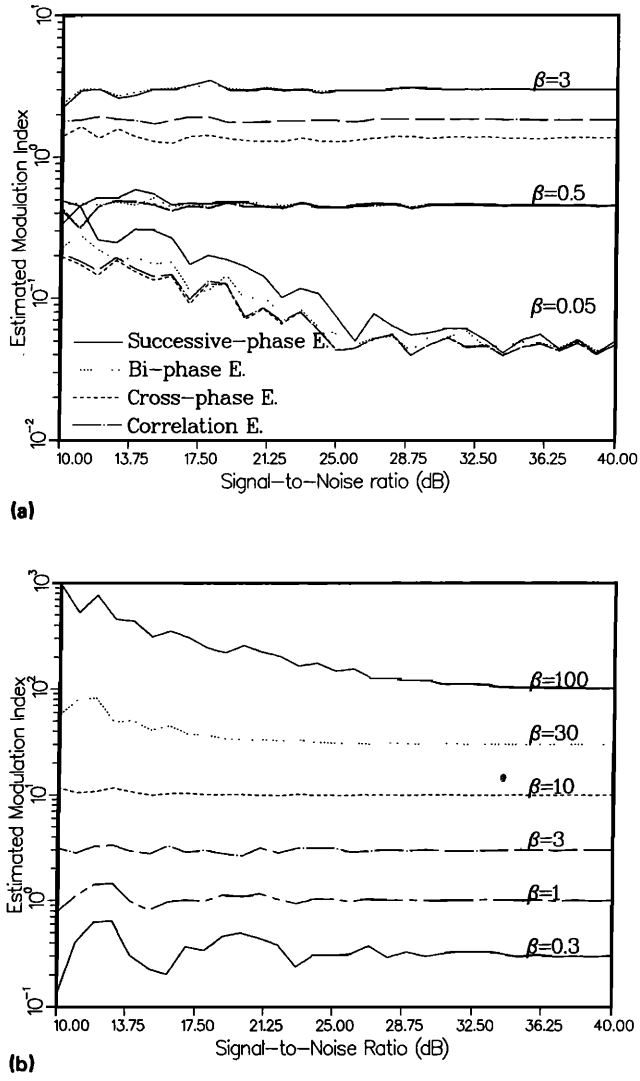

FIG. 3. (a) Estimated modulation index against signal-to-noise ratio for four different algorithms: $\hat{\beta}_1, \hat{\beta}_2, \hat{\beta}_3$, and $\hat{\beta}_4$. True modulation indices are $\beta = 3$, 0.5, and 0.05 from top to bottom, and the sampling frequency is $f_s = 6f_L$ in each case; (b) wide applicable range for the successive-phase estimator $\hat{\beta}_1$ with true modulation indices $\beta = 0.3$, 1, 3, 10, 30, and 100 and sampling frequency $f_s = 2.4\beta f_L$ in each case.

B. Applicable range of vibration amplitude estimation

Since the power spectrum of the pure-tone FM signal is a Fourier–Bessel series with harmonics spacing at the modulation frequency f_L,[27] the sampling frequency must be high enough to include the first few spectral harmonics without aliasing. From our experience in simulation, the minimum sampling frequency must be at least four times higher than the vibration frequency (or modulation frequency) to achieve satisfactory estimation. Aside from this general sampling criterion, there are different sampling criteria for each estimator. For the successive-phase estimator in Eq. (15), the phase signal is derived from the arctangent function and has a basic range limitation

$$0 \leqslant |\phi_k| = 2\beta \left| \cos\left(k\omega_L T_s - \frac{\omega_L T_s}{2}\right) \sin\left(\frac{\omega_L T_s}{2}\right) \right| \leqslant \pi. \tag{49}$$

Since the cosine term is always less than 1, the above expression can be simplified as

$$2\beta \left|\sin(2\pi f_L / 2f_s)\right| \leqslant \pi. \tag{50}$$

If the sampling frequency is high, the small argument approximation for the sine function can be made. Then, the following sampling restriction can be derived:

$$f_s \geqslant 2\beta f_L. \tag{51}$$

This is the sampling criterion chosen in Fig. 3(b). In practice, the maximum modulation index can be estimated from the strength of the vibration source, and then the sampling frequency can be determined accordingly. The same sam-

pling criterion applies for the successive-co-phase estimator in Eq. (16), biphase estimator in Eq. (17), and cross-phase estimators in Eqs. (18), (19), and (15), where the phase and co-phase signals are used. But for those estimators, since the trigonometric function to be approximated is the cosine function instead of the sine function, there is a limitation of the maximum estimatable modulation index $\beta_{\max}$:

$$\beta_{\max} \lesssim \pi/2. \tag{52}$$

If this rule is violated, the aliasing of the phase will occur, which will subsequently lead to the aliasing of the modulation index β (or the vibration amplitude).

For the minimum estimatable modulation index $\beta_{\min}$, however, good estimation can always be achieved with high signal-to-noise ratio in simulation. As a rule of thumb, the minimal estimatable modulation index as function of signal-to-noise ratio and sampling frequency can be described as

$$\log_{10}(1/\beta_{\min}) \gtrsim \mathrm{SNR}_{\mathrm{dB}}/10\ (f_s/f_L)^{0.5}. \tag{53}$$

This rule of thumb also applies to biphase and cross-phase estimators, and applies especially well to correlation estimators which exploit small argument expansion for the zeroth-order Bessel function.

Figure 4 is a summary of the range of validity of each estimator. The lower axis is an example of a typical sonoelasticity imaging application using ultrasound as the interrogating wave with the following parameters: $f_0 = 7.5$ MHz, $c_0 = 1500$ m/s, $\lambda_0 = 0.2$ mm, and $\theta = 10°$. In this graph of applicable range of estimation, the upper limit of the successive-phase estimator and the lower limit of the correlation estimators are depicted roughly by Eqs. (51) and (53), respectively.

C. Effects of nonlinearity on vibration amplitude estimation

In practical applications, the vibration is not always pure-tone sinusoid because of some medium or vibration source nonlinearities. In this case, assuming that only fundamental and the second harmonics are significant in the vibration, then the returned signal can be written as

$$s_r(t) = A\cos[\omega_0 t + \beta\sin(\omega_L t + \varphi_1) + \beta_2\sin(2\omega_L t + \varphi_2)], \tag{54}$$

where β and β_2 are the modulation indices of the fundamental and second harmonics of the vibration, respectively. The nonlinearity can be defined as

$$N_2 \equiv \beta_2/\beta \times 100\%. \tag{55}$$

For small nonlinearity (less than 10%), the performance of all estimators are essentially not affected as shown in Fig. 5 where a noise-free signal is analyzed. The sampling frequency is held constant at $f_s = 6f_L$ and the true modulation index is $\beta = 0.5$ for all estimations. Note that the cross-phase estimator and correlation estimators show almost zero estimation errors. Even in the worst case of 10% nonlinearity, the phase estimator only introduces less than 1.2% estimation error. Thus we can conclude that all these time domain estimators are insensitive to the nonlinearity.

D. Vibration frequency estimation

An unknown vibration frequency can be estimated in several ways. Equation (21) provides one easy way to obtain the estimation. Figure 6 shows the performance of this phase-ratio estimator against vibrational cycles. Signal-to-noise ratio is maintained at 30 dB, the modulation index is $\beta = 1.2$, and the sampling frequency is fixed at $f_s = 5.436f_L$ for simulations at three different vibration frequencies $f_L = 100$, 250, and 400 Hz in Fig. 6. The results indicate that the phase of the vibration has little effect on the frequency estimation. The deviation is approximately proportional to the vibration frequency since the first estimated parameter is the tangent function of the product of the vibration frequency and the sampling frequency.

III. CONCLUSION

Five time domain estimators (and variations) are presented in this paper. Four of them estimate the modulation index (or equivalently the vibration amplitude), and the other one estimates the vibration frequency. The successive-phase estimator in Eq. (15) covers a broad range of the esti-

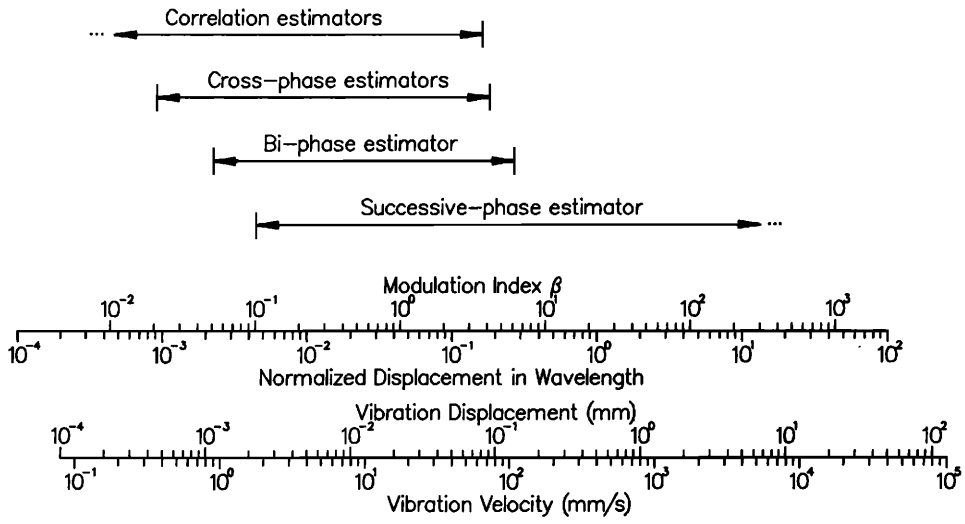

FIG. 4. The applicable range for the time domain estimation algorithms discussed in the text. The relation of modulation index and the normalized estimated vibration amplitude of displacement field is plotted. Two auxiliary axes are drawn for the typical sonoelasticity application where the parameters of the interrogating wave are $f_0 = 7.5$ MHz, $c_0 = 1500$ m/s, $\lambda_0 = 0.2$ mm, and $\theta = 10°$.

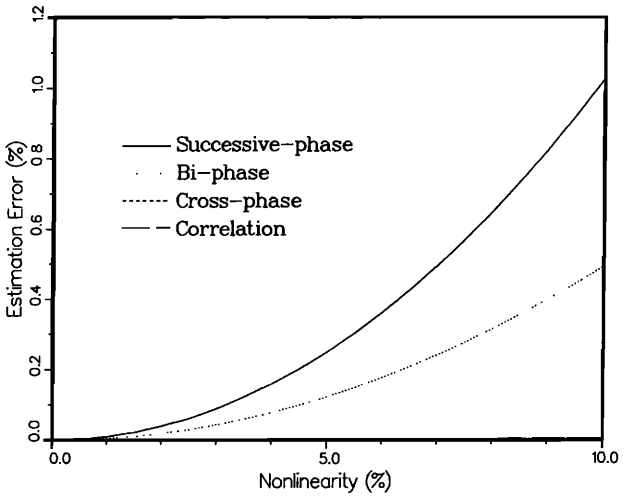

FIG. 5. Percentile estimation errors (noise-free) against nonlinearity for four vibration amplitude estimators: $\hat{\beta}_1$, $\hat{\beta}_2$, $\hat{\beta}_3$, and $\hat{\beta}_4$. True modulation index is $\beta = 0.5$ and the sampling frequency is $f_s = 6f_L$. Since the estimation errors for $\hat{\beta}_3$ and $\hat{\beta}_4$ are so small, their percentile error curves are overlapped with the horizontal axis.

mated parameter. The upper limit of valid estimation depends on the sampling frequency. The required calculation is also minimal and simplest among all estimators discussed. The successive-co-phase estimator in Eq. (16) is a variant of the successive-phase estimator and has almost the same performance as the successive-phase estimator. The biphase estimator in Eq. (17) uses both phase and co-phase signals; thus it has better performance than the successive-phase estimator when the modulation index β is small. Noise performance is improved with cross-phase estimators [Eqs. (18), (19)] but the estimation range is reduced. The n-shift-cross-phase estimator in Eq. (15) is also the most flexible one for the design of the image scanning system. Sampling criteria as shown in Eqs. (52), (51), and (53) must be followed to maintain good estimation.

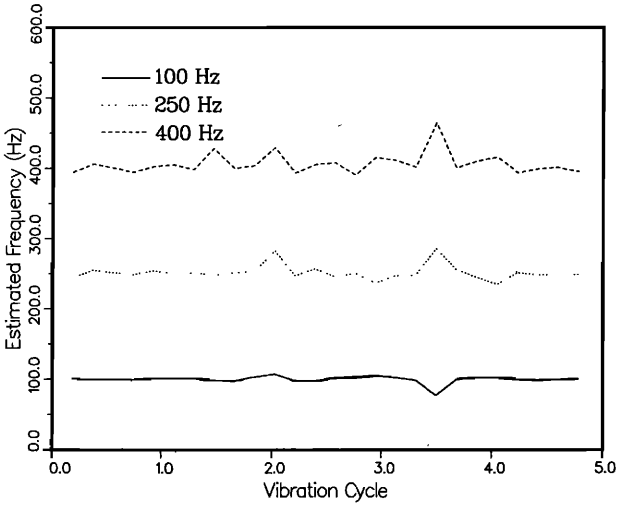

FIG. 6. Three different vibration frequencies ($f_L = 400$, 250, and 100 Hz from top to bottom) are estimated by the phase-ratio estimator $\hat{f}_L$. Five cycles of vibration are shown on the graph. Signal-to-noise ratio is 30 dB, the true modulation index is $\beta = 1.2$, and the sampling frequency is $f_s = 5.436f_L$.

Correlation estimators [the autocorrelation estimator in Eq. (32), the quasiautocorrelation estimator in Eq. (38), and the dual-autocorrelation estimator in equation (39)] provide alternative approaches when the vibration amplitude is small. The minimum estimatable vibration amplitude is determined by the system noise and sampling criterion given in Eq. (53). The length of the sequence used in the correlation estimators is adjustable and is a parameter in making an image. Carefully choosing the correlation length will be helpful in producing good real-time images.

The phase-ratio estimator in Eq. (21) estimates the vibration frequency. Since the vibration frequency used in real applications is expected to be constant or slowly changing, the estimation can be improved significantly by simple filtering. As long as the vibration frequency estimation is maintained in a certain range of accuracy, the vibration amplitude can then be accurately estimated using one of the algorithms described above.

Furthermore, either phase estimators or correlation estimators can be implemented using rf signals. This alleviates the restriction of requirements for signal processing and electronic circuitry. Trade-offs between signal processing and electronic circuitry can be made accordingly.

Also, conventional Doppler techniques can be modified to estimate the vibration parameters. However, if the deterministic property of the sinusoidal vibration is not used, the final estimate will suffer from the finite truncation and nonzero initial phase.

All of the time-domain estimators proposed in this paper make use of *a priori* knowledge of vibration, and, therefore, require only a small fraction of the vibration cycle and a minimum of two samples to estimate the desired parameters. Furthermore, the resulting estimations are not affected substantially by the vibration phase. Together with the frequency domain estimators developed in our previous paper,[19] they cover a wide working range of signals and working conditions (e.g., sampling criteria, vibration amplitude, noise level, and nonlinearity). Therefore, they are useful in various real-time imaging and remote sensing applications in radar, sonar, and acoustics.

ACKNOWLEDGMENT

This work was supported by the University of Rochester, Department of Electrical Engineering, during an era when many funding agencies were pursuing their own agendas.

[1] D. W. Baker, "Pulsed Doppler blood flow sensing," IEEE Trans. Sonics Ultrason. **SU-17** (3), 170–185 (1970).
[2] B. A. Coghlan and M. G. Taylor, "Directional Doppler techniques for detection of blood flow," Ultrasound Med. Biol. **2**, 181–188 (1976).
[3] M. Brandestini, "Topoflow—A digital full-range Doppler velocity meter," IEEE Trans. Sonics Ultrason. **SU-25** (5), 287–293 (1978).
[4] B. A. J. Angelsen and K. Kristoffersen, "On ultrasonic MTI measurement of velocity profiles in blood flow," IEEE Trans. Biomed. Eng. **BME-26** (12), 665–671 (1979).
[5] L. Gerzberg and J. D. Meindl, "Power spectrum centroid detection for Doppler systems applications," Ultrason. Imag. **2**, 232–261 (1980).
[6] B. A. J. Angelsen, "Instantaneous frequency, mean frequency, variance of mean frequency estimators for ultrasonic blood velocity Doppler signals," IEEE Trans. Biomed. Eng. **BME-28** (11), 733–741 (1981).
[7] B. A. J. Angelsen, "Discrete time estimation of the mean Doppler frequency in ultrasonic blood velocity measurements," IEEE Trans.

Biomed. Eng., **BME-30**, 207–214 (April 1983).
[8] C. Kasai, K. Namekawa, A. Koyano, and R. Omoto, "Real-time two-dimensional blood flow imaging using an autocorrelation technique," IEEE Trans. Sonics Ultrason. **SU-32**, 458–463 (May 1985).
[9] W. D. Barber, J. W. Eberhard, and S. G. Karr, "A new time domain technique for velocity measurements using Doppler ultrasound," IEEE Trans. Biomed. Eng. **BME-32**, 213–229 (March 1985).
[10] K. Kristoffersen and B. A. J. Angelsen, "A comparison between mean frequency estimators for multigated Doppler systems with serial signal processing," IEEE Trans. Biomed. Eng. **BME-32** 9, 645–657 (1985).
[11] O. Bonnefous, P. Pesque, and X. Bernard, "A new velocity estimator for color flow mapping," in IEEE Ultrason. Symp. **2**, 855–858 (1986).
[12] K. Kristoffersen, "Time-domain estimation of the center frequency and spread of doppler spectra in diagnostic ultrasound," IEEE Trans. Ultrason. Ferroelec. Freq. Control **UFFC-35** (4), 484–497 (1988).
[13] L. Y. L. Mo, L. C. M. Yun, and R. S. C. Cobbold, "Comparison of four digital maximum frequency estimators for Doppler ultrasound," Ultrasound Med. Biol. **14** (5), 355–363 (1988).
[14] R. M. Lerner and K. J. Parker, "Sono-elasticity images," in *Ultrasonic Tissue Characterization and Echographic Imaging*, Proceedings of the 7th European Communities Workshop, Nijmegen, The Netherlands, October 1987 (UECOM, Luxemborg, 1987).
[15] R. M. Lerner, K. J. Parker, J. Holen, R. Gramiak, and R. C. Waag, "Sono-elasticity: Medical elasticity images derived from ultrasound signals in mechanically vibrated targets," in *Acoustic Imaging*, edited by L. W. Kessler (Plenum, NY, 1988), Vol. 16, pp. 317–327.
[16] R. M. Lerner, S. R. Huang, and K. J. Parker, "Sonoelasticity images derived from ultrasound signals in mechanically vibrated tissues," Ultrasound Med. Biol. **16** (3), 231–239 (1990).
[17] K. J. Parker, S. R. Huang, R. A. Musulin, and R. M. Lerner, "Tissue response to mechanical vibrations for sonoelasticity imaging," Ultrasound Med. Biol. **16** (3), 241–246 (1990).
[18] J. Holen, R. C. Waag, and R. Gramiak, "Representations of rapidly oscillating structures on the Doppler display," Ultrasound Med. Biol. **11**, 267–272 (1985).
[19] S. R. Huang, R. M. Lerner, and K. J. Parker, "On estimating the amplitude of harmonic vibration from the Doppler spectrum of reflected signals," J. Acoust. Soc. Am. **88**, 2702–2712 (1990).
[20] K. J. Taylor, "Absolute measurement of acoustic particle velocity," J. Acoust. Soc. Am. **59**, 691–694 (1976).
[21] K. J. Taylor, "Absolute calibration of microphone by a laser Doppler," J. Acoust. Soc. Am. **70**, 939–945 (1981).
[22] J. Jarzynski, D. Lee, J. Vignola, Y. H. Berthelot, and A. D. Pierce, "Fiber optics Doppler systems for remote sensing of fluid flow," in *Ocean Optics IX, Proceedings of SPIE Conference on Optics, Electro-Optics, and Sensors*, 4–6 April 1988 (SPIE, Bellingham, WA, 1988), Vol. 925, pp. 250–254.
[23] M. Cox, and P. H. Rogers, "Automated noninvasive motion measurement of auditory organs in fish using ultrasound," J. Vib., Acoust. Stress Reliability Design **109**, 55–59 (January 1987).
[24] Y. Yamakoshi, J. Sato, and T. Sato, "Ultrasonic imaging of internal vibration inside of soft tissue under forced vibration," IEEE Trans. Ultrason. Ferroelec. Freq. Control **UFFC-37**, 45–53 (March 1990).
[25] D. Censor, "Acoustical Doppler effect analysis—Is it a valid method?," J. Acoust. Soc. Am. **83**, 1223–1230 (1988).
[26] J. C. Piquette, A. L. V. Buren, and P. H. Rogers, "Censor's acoustical Doppler effect analysis—Is it a valid method?," J. Acoust. Soc. Am. **83**, 1681–1682 (1988).
[27] A. B. Carlson, *Communications Systems* (McGraw Hill, New York, 1986), Chap. 8, pp. 221–227.
[28] G. N. Watson, *Treatise on the Theory of Bessel Functions* (MacMillan, New York, 1945), Chap. 2, pp. 14–15, 31.
[29] D. Middleton, *Introduction to Statistical Communication Theory* (McGraw-Hill, New York, 1960), Chap. 14, pp. 599–635.
[30] H. L. van Trees, *Detection, Estimation, and Modulation Theory* (Wiley, New York, 1971), part III, pp. 576–578.
[31] S. M. Kay and J. S. L. Marple, "Spectrum analysis—a modern perspective," Proc. IEEE **69**, 1380–1419 (1981).